

Identification of Λ -like systems in $\text{Er}^{3+}:\text{Y}_2\text{SiO}_5$ and observation of electromagnetically induced transparency

E. Baldit, K. Bencheikh,^{*} P. Monnier, S. Briaudeau,[†] and J. A. Levenson
Laboratoire de Photonique et de Nanstructures, CNRS-UPR 20, 91460 Marcoussis, France

V. Crozatier, I. Lorgeré,[‡] F. Bretenaker, and J. L. Le Gouët
Laboratoire Aimé Cotton, CNRS-UPR 3321, University Paris-Sud, Bât. 505, 91405 Orsay Cedex, France

O. Guillot-Noël[‡] and Ph. Goldner
*Laboratoire de Chimie de la Matière Condensée de Paris, CNRS-UMR 7574, ENSCP,
 11 rue Pierre et Marie Curie, 75231 Paris Cedex 05, France*

(Received 5 February 2010; published 30 April 2010)

Electromagnetically induced transparency (EIT) is reported in a solid-state material doped with erbium ions. In this paper we introduce the spectroscopic investigations we have conducted in order to identify the adequate Λ -like three-level systems in $\text{Er}^{3+}:\text{Y}_2\text{SiO}_5$ crystal, relevant for the demonstration of EIT. These results pave the way for nonlinear and quantum optics applications based on EIT at the telecom wavelength around $1.5 \mu\text{m}$.

DOI: [10.1103/PhysRevB.81.144303](https://doi.org/10.1103/PhysRevB.81.144303)

PACS number(s): 78.47.nd, 32.80.Qk, 42.50.Gy

I. INTRODUCTION

Electromagnetically induced transparency (EIT) is a well-known quantum interference phenomenon allowing the annihilation of the absorption of an otherwise absorbing medium when excited with a resonant electromagnetic field.¹ Beyond this linear effect, EIT has been during the last years a master phenomenon for a wide variety of applications in nonlinear and quantum optics. EIT has indeed been reported in atomic vapors, cold atoms, and also in solids and allowed the enhancement of nonlinear optical processes, slow light propagation, and storage of optical pulses (for a review, see, for example, Ref. 1). More recently storage of squeezed states of light has been demonstrated by two groups,^{2,3} showing the exciting potential of EIT for quantum states manipulation and quantum information.

The standard configuration for EIT is a three-level Λ -like system excited by two electromagnetic fields labeled coupling and probe, sharing a common excited state and starting from distinct ground levels. Generally, the efficiency of EIT is dictated by the lifetime and the coherence of the ground levels. In the quest of such system with outstanding performance, rare-earth ion-doped crystals are expected to play an important role. In such solid-state materials, the triply ionized rare-earth ions are characterized by fine optical transitions among $4f^n$ electrons shielded from the crystalline environment by the outer $5s$ and $5p$ electrons. This confers to the ions a long-lived excited electronic state where T_1 can range from microsecond to millisecond. T_1 can even be longer for the hyperfine levels, depending on the process involved in the population redistribution among the hyperfine sublevels of the ground electronic state.⁴ In addition, the optical and hyperfine coherences T_2 can be extended through a careful choice of the host material in order to minimize the perturbation induced by the host atoms on the rare-earth ions and through the concentration of the rare-earth ions in the crystal in order to reduce the mutual interaction between the closest

rare-earth ions. Fraval *et al.*⁵ succeeded to extend the coherence time of the hyperfine transitions in a praseodymium-doped Y_2SiO_5 crystal to about 30 s by applying an appropriate magnetic field and a rf pulse sequence, reducing the spin fluctuations and storing light more than 1 s using EIT in the same material.⁶ More recently, by embedding the praseodymium in a different host material, the $\text{La}_2(\text{WO}_4)_3$ crystal, Goldner *et al.*⁷ have measured a coherence time of 250 μs and observed efficient EIT. Erbium-doped systems are popular for applications in several domains mainly due to the fact that the optical transition occurs around $1.5 \mu\text{m}$ coinciding with the transparency band of telecom optical fibers. Erbium-doped crystals were used in many coherent nonlinear interactions including ultraslow light propagation via coherent population oscillations.⁸ Oddly enough, EIT was not yet reported in erbium-doped materials. This demonstration is the main achievement reported in this paper.

In our investigations, we have adopted the Y_2SiO_5 crystal as the host material. This crystal lattice has been chosen because it engenders very low perturbation on the rare-earth ions when working at low temperatures. Indeed, long coherence times are expected because the constituent elements in Y_2SiO_5 have small magnetic moments ($-0.137\mu_N$ for ^{89}Y) or small natural abundance of magnetic isotopes (4.7% with $-0.554\mu_N$ for ^{29}Si and 0.04% with $-1.89\mu_N$ for ^{17}O). By a careful choice of the erbium ions concentration and by applying an appropriate external magnetic field to the crystal, Böttger⁹ achieved a dephasing time of 4.38 ms in Y_2SiO_5 crystal doped with natural erbium ions, showing the possibility of manipulating and increasing the coherence. All this, along with the work in Ref. 5, suggest that the manipulation of the hyperfine coherence in erbium-doped Y_2SiO_5 crystal can be achieved, putting this solid-state material as a promising candidate for EIT and the subsequent applications in the telecom wavelength range.

In our approach, we have besides particularly chosen the isotope 167 for its nuclear spin $I=7/2$ which is at the origin

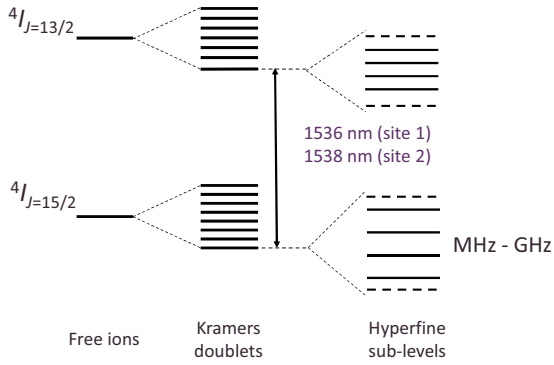


FIG. 1. (Color online) Energy levels of erbium ions.

of a rich hyperfine structure among which at least two Λ -like systems with optical transitions at $1.5 \mu\text{m}$ have been identified and in which EIT has been observed. This paper describes first the spectroscopic investigations we have conducted in order to characterize the unknown hyperfine structure of the $^{167}\text{Er}^{3+}$ ions in the particular crystal Y_2SiO_5 and to identify Λ -like three-level systems suitable for EIT. In Sec. II, we describe the spectral hole burning (SHB) spectroscopy, a technique used along with electron-paramagnetic-resonance (EPR) spectroscopy for the identification of the energy-level structure of the erbium ions. Among these levels, two Λ -like systems have been identified. Section III is dedicated to what we believe is the first experimental demonstration of EIT in the erbium-doped crystal.

II. IDENTIFICATION OF Λ -LIKE SYSTEMS

A. $\text{Er}^{3+}:\text{Y}_2\text{SiO}_5$ crystal

The crystal used in our experiments is an yttrium oxyorthosilicate (Y_2SiO_5) lattice doped with 0.005 at. % of $^{167}\text{Er}^{3+}$ ions supplied by Scientific Materials Inc. (Bozeman, Montana). It is cut along the three orthogonal optical extinction axes \mathbf{b} (3 mm), \mathbf{D}_1 (5 mm), and \mathbf{D}_2 (6 mm). The Y_2SiO_5 has a monoclinic structure with $C2/c$ space group. The Er^{3+} ions substitute to yttrium ions in two nonequivalent low-symmetry C_1 sites surrounded, respectively, by seven and six neighbors. The energy diagram of the erbium ions is depicted in Fig. 1. The free erbium ions have a $4f^{11}$ configuration with $^4I_{15/2}$ being the ground state and $^4I_{13/2}$ being the first excited state, where 15/2 and 13/2 are the total momenta $J=L+S$. Under the influence of the electric field produced by the crystalline environment, the degeneracy of the $J=15/2$ level is partially lifted and the level splits into eight Kramer's doublets. Equivalently, the excited state $J=13/2$ splits into seven Kramer's doublets. At liquid-helium temperature, only the lowest Kramer's doublet of the ground state $^4I_{15/2}$ is populated and it can be described by an effective electronic spin $S_{\text{eff}}=1/2$. The transition wavelength from the lowest Kramer's doublet of the ground state $^4I_{15/2}$ to the lowest Kramer's doublet of the excited state $^4I_{13/2}$ is 1536 nm for erbium ions in site 1 and 1538 nm for those in site 2.

Among the erbium isotopes, we choose $^{167}\text{Er}^{3+}$ ions, the only isotope having a nuclear spin that is $I=7/2$. Due to the hyperfine interaction $H_{\text{hyp}}=\mathbf{S}\cdot\mathbf{A}\cdot\mathbf{I}$ and the quadrupole inter-

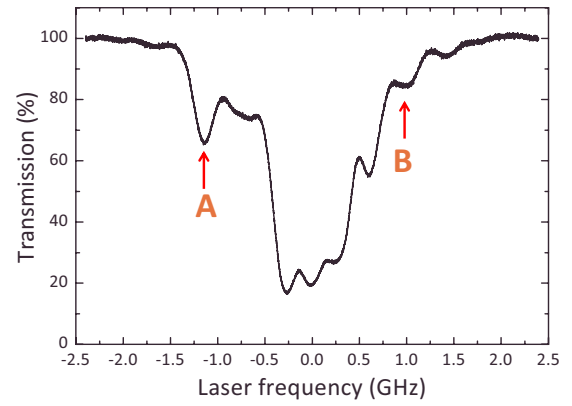


FIG. 2. (Color online) Linear transmission of a weak electromagnetic field across a 3-mm-long $^{167}\text{Er}^{3+}:\text{Y}_2\text{SiO}_5$ crystal. The wavelength is tuned around 1536 nm in order to excite the erbium ions in site 1. The crystal is maintained at low temperature (1.5 K).

action $H_q=\mathbf{I}\cdot\mathbf{Q}\cdot\mathbf{I}$, where \mathbf{A} and \mathbf{Q} are, respectively, the hyperfine matrix and the electric quadrupole matrix, the Kramer's doublets split into maximum $(2S_{\text{eff}}+1)(2I+1)=16$ hyperfine sublevels even in the absence of any external magnetic field because of the low symmetry of the crystal. The matrix \mathbf{A} and \mathbf{Q} of the ground state $^4I_{15/2}$ have been fully determined using the EPR spectroscopy.¹⁰ The huge number of hyperfine sublevels in the excited and ground states offers in principle multiple possibilities of Λ -like schemes for EIT. Indeed, all the transitions are allowed because the selection rule is not fulfilled as the hyperfine levels are not pure quantum states but mixtures of $|I=7/2, M_I\rangle$, where $M_I = \pm 7/2, \pm 5/2, \pm 3/2, \pm 1/2$ is the projection of the nuclear spin.

Identifying these Λ -like systems is a challenging task essentially because the hyperfine structure is hidden by the inhomogeneous broadening associated with the inhomogeneity of the crystal field. Figure 2 shows the linear transmission at 1.5 K of a weak electromagnetic field tuned over few gigahertz in order to cover all the inhomogeneously broadened transition of erbium ions in site 1 ($\lambda=1536$ nm). The electromagnetic field propagates along axis \mathbf{b} of the crystal and is linearly polarized along \mathbf{D}_2 axis. The $^{167}\text{Er}^{3+}:\text{Y}_2\text{SiO}_5$ transmission shows peaks that are convolution of the inhomogeneous broadening with some of the hyperfine transitions. The number of hyperfine transitions is expected to be higher than the few peaks appearing in the spectrum depicted in Fig. 2. This disagreement between the theoretical expectations and the experimentally observed peaks is due to the rather large inhomogeneous linewidth (few hundreds of megahertz) masking the smallest hyperfine splittings.

B. Spectral hole burning spectroscopy

In order to determine the unresolved hyperfine splittings hidden by the inhomogeneous broadening, SHB spectroscopy is used.^{4,11} In this technique, a pump field whose frequency is fixed within the inhomogeneous absorption line excites those particular ions whose energy difference between any hyperfine ground state and any hyperfine excited

state coincides with the pump frequency. In the $^{167}\text{Er}^{3+}:\text{Y}_2\text{SiO}_5$, there are 256 (16×16) possible ion classes that can fulfill the resonance condition. In the stationary regime, each class of ions sees the population of its hyperfine ground state concerned by the pumping process, depleted and transferred to the other remaining 15 hyperfine levels.

A weak electromagnetic field called probe can read this population redistribution by measuring its absorption as its frequency is tuned over the whole inhomogeneous line. Indeed to the depleted hyperfine ground state are associated holes (less absorption) in the absorption profile, whereas antiholes (more absorption) are associated with transitions involving the overpopulated hyperfine ground states. The linewidths of these holes and antiholes are on the order of the homogeneous broadening. It is by measuring the frequency separations of these holes and antiholes from the pump frequency that the hyperfine splittings of the ground and excited states can be inferred. A simple analysis shows that the splittings among the excited hyperfine sublevels are inferred from the holes whereas the antiholes are linear combinations of the splittings of both the ground and excited hyperfine sublevels. This situation is true when the inhomogeneous broadening is much larger than any hyperfine splitting and thus when all the ions classes are excited. In this case the number of holes and antiholes is independent on where the pump is positioned in the inhomogeneous line. However this is not the case for $^{167}\text{Er}^{3+}:\text{Y}_2\text{SiO}_5$ where the different splittings can be smaller or larger than the inhomogeneous broadening. This situation is very complicated since only a fraction of ion classes, dependent on the pump wavelength, is excited and thus the holes and antiholes structures vary depending on where the pump frequency is fixed in the inhomogeneous line.

Despite the complexity of the system, some of the hyperfine sublevels have been identified using SHB spectroscopy and are consistent with the ground-state hyperfine structure fully identified using EPR spectroscopy.¹⁰ Note that for EIT, it is not necessary to know the entire hyperfine structure of the excited state. Indeed, what is relevant is the knowledge of the splitting of two hyperfine sublevels of the ground state that will form a Λ system with any hyperfine sublevel of the excited state.

The experimental setup for the SHB spectroscopy is depicted in Fig. 3. The pump source is a continuous-wave (cw) Er-doped fiber laser (KOHERAS) emitting about 5 mW at 1536 nm and temperature tunable by about 1 nm. The probe source is an Er-doped fiber laser purchased from KOHERAS as well. It is a cw 2 kHz linewidth laser emitting more than 150 mW at 1536 nm. It is possible to slowly tune it by changing the fiber temperature and faster (500 Hz bandwidth) by pulling the laser fiber using a PZT transducer that is externally controlled with a wave-function generator (SRS DS345). The overall tunability is 1 nm. Acousto-optic modulators (AOMs) on the optical paths of pump and probe fields are used to gate the pump and the probe beams, to control their durations, and their relative delay. The AOMs are driven by a digital pulse/delay generator (SRS DG535). The probe field is then detected using an InGaAs detector (New Focus 1181). In order to improve the signal-to-noise ratio (SNR) of the detection, frequency modulation (FM) tech-

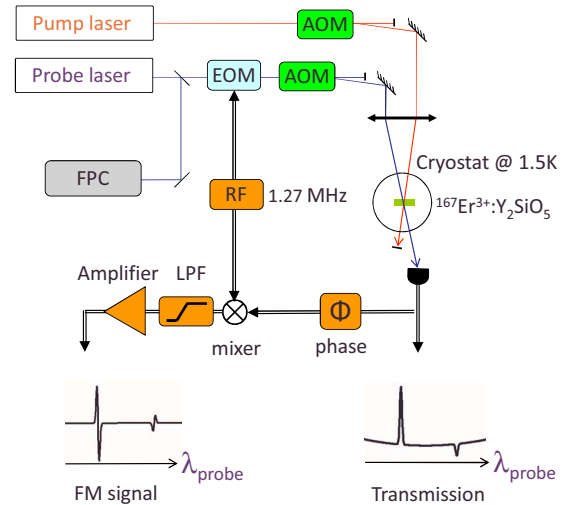


FIG. 3. (Color online) Scheme of the experimental setup for spectral hole burning spectroscopy. FPC: Fabry-Perot cavity used as a frequency reference. The free spectral range is 300 MHz; EOM: electro-optic modulator; AOM: acousto-optic modulator; LPF: low-pass filter; and Φ is an adjustable electronic phase in order to optimize the FM signal.

nique is implemented.¹² For this purpose, the probe field is phase modulated using an electro-optic modulator (EOM) driven at 1.27 MHz. We are able to obtain an FM signal of the transmitted probe having an improved SNR by a factor of 10 with respect to the SNR of the direct transmission signal. Both the direct transmission and the FM signal are acquired with a 500 MS/s sampling rate numerical oscilloscope.

A square-shaped 20 ms long pump pulse is first applied to the crystal. The central wavelength of the pulse is fixed within the inhomogeneous line of the crystal. Its peak power is about 1.7 mW and its waist is 680 μm . After a delay that can be varied at will, the probe pulse is applied. Its duration is 1 ms and its frequency is linearly tuned over few hundreds of megahertz within the inhomogeneous line. The probe beam is focused down to a waist of 377 μm . Its peak power is weak, about 10 μW , in order to avoid bleaching. The frequency of the probe is swept at a 200 Hz rate using a triangle shaped signal delivered by a wave generator driving the PZT of the laser.

Typical probe transmission and FM signals are depicted in Fig. 4 as the probe frequency is tuned. They show a huge number of holes and antiholes which makes it rather difficult to extract the hyperfine structure of the ground and excited states. Nevertheless, exploiting spectra similar to those in Fig. 4 for a series of pump wavelength exploring the inhomogeneous line and along with the EPR spectroscopy results,¹⁰ we were able to identify about ten interesting configurations corresponding to Λ -like systems. Two of them have been addressed in order to implement EIT. Both are shown in Fig. 5 along with the hyperfine structure of the ground electronic state $^4I_{15/2}$. The first one is obtained when the pump frequency is fixed in the inhomogeneous line at A as indicated by the arrow in Fig. 2. When the probe is tuned to the blue, 880 MHz away from the pump, an antihole appears, revealing a transfer of population from the hyperfine

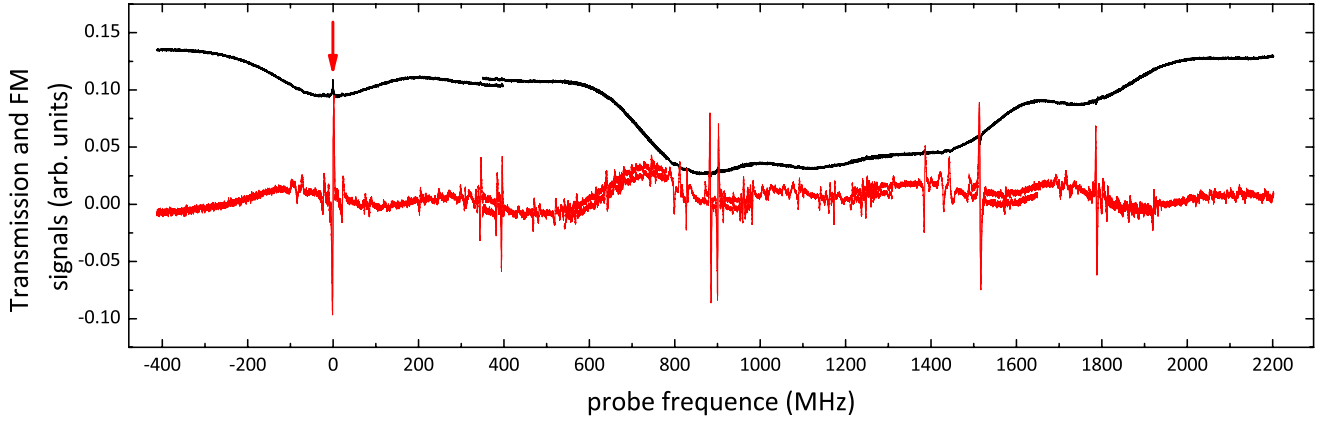


FIG. 4. (Color online) Top (black): transmission of a weak probe tuned around 1536 nm as erbium ions are excited by the pump indicated by the red arrow. Bottom (red): FM signal associated with the probe transmission. The presence of holes and antiholes is revealed in the FM signal by the dispersive shapes having slopes with opposite signs.

sublevel $|4\rangle$ to sublevel $|3\rangle$). The interval between the states is in agreement with the EPR results.¹⁰ When the frequency of the pump is at B (see arrow in Fig. 2), a red detuned antihole peak appears in the transmission profile of the probe at 740 MHz away from the pump frequency, revealing this time a population transfer from hyperfine sublevel $|1\rangle$ to sublevel $|2\rangle$. We notice in both cases that one expect EIT effect to be superposed to the pumping effect, so the EIT transmission peak grows up inside the antihole. We also draw attention on the fact that the two Λ -like systems are not associated with

the same ions class since the splitting of states $|1\rangle$ and $|4\rangle$ is about 5.6 GHz, whereas the splitting between A and B inferred from Fig. 2 is about 2.5 GHz.

The EIT amplitude and width are governed by both the hyperfine coherence and the population in the hyperfine sublevel excited by the probe field. Ideally, the coherence lifetime should be infinite and all the population in the hyperfine sublevel resonant with the probe, whereas the hyperfine sublevel excited by the pump field should remain empty. In order to approach this configuration, we have investigated the

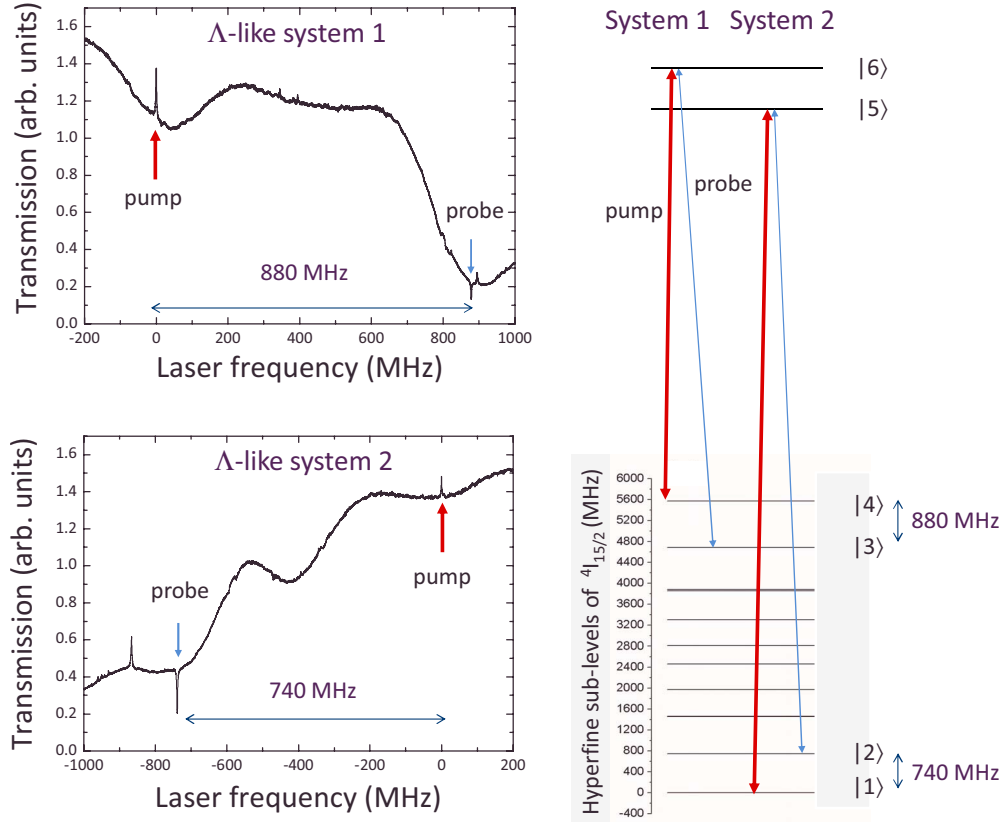


FIG. 5. (Color online) Left: transmission of the probe with the pump applied at two different positions indicated by the red arrow in the inhomogeneous line. Right: hyperfine structure of the electronic ground state $^4I_{15/2}$ and the two identified Λ -like systems.

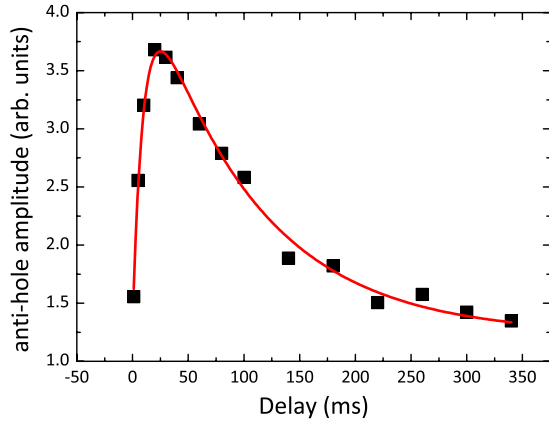


FIG. 6. (Color online) Evolution of the antihole amplitude as the delay between the pump and the probe pulse is varied. The solid line is a second-order exponential decay fit with time constants 10 and 97 ms.

population transfer from the hyperfine sublevel excited by the pump to the one excited by the probe using the optical pumping effect. For this purpose we have measured the evolution of the amplitude of the antiholes in both systems which is an indication of the population of the ions in the hyperfine sublevel $|3\rangle$, for system 1, and sublevel $|2\rangle$ for system 2.

First, both systems are excited by a 60 ms square pump pulse. After a delay τ , a weak probe pulse is applied. Its frequency is tuned around the antihole. Figure 6 shows for system 1 the evolution of the amplitude of the antihole as the delay between the pump pulse and the probe pulse is varied. A maximum antihole amplitude is reached for a delay $\tau \approx 28$ ms, at which the population in the probe hyperfine sublevel reaches a maximum value. The evolution of the antihole amplitude is driven by two-time constants: the excited state lifetime T_1^{opt} and the population relaxation time T_1^{hyp} among the hyperfine sublevels of the ground state. The continuous line in Fig. 6 is a second-order exponential fit with time constants $T_1^{opt}=10$ ms and $T_1^{hyp}=97$ ms. The optical lifetime $T_1^{opt}=10$ ms is consistent with values reported in Ref. 13 and gives a confidence on the value of the hyperfine lifetime.

III. ELECTROMAGNETICALLY INDUCED TRANSPARENCY

Electromagnetically induced transparency is implemented in the two Λ -like systems identified by SHB spectroscopy and EPR spectroscopy. Both systems are formed by two hyperfine sublevels of the ground state and a hyperfine sublevel of the excited state. In order to achieve EIT, the coupling and the probe fields should simultaneously excite the Λ -like systems. For this purpose, both fields are generated by the same laser as depicted in Fig. 7. The source we use is the one labeled probe in the SHB spectroscopy experiment in Sec. II B. The laser beam is first split into an 80% and a 20% relative intensity beams in order to obtain pump/coupling and probe, respectively. The frequency detuning ν_{rf} between

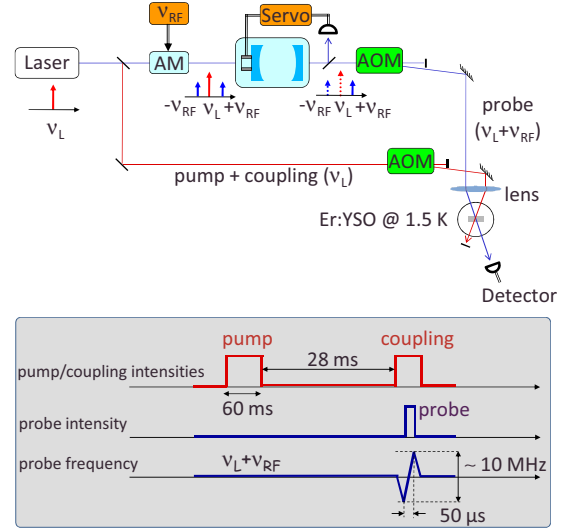


FIG. 7. (Color online) Scheme of the experimental setup used to observe EIT. In the gray box are indicated the pulse sequences applied to the AOMs in order to control the intensities and the duration of the pump, control, and probe pulses. The fine frequency tuning of the probe frequency is achieved by changing the RF frequency of the AOM in the optical path of the probe.

the coupling and the probe corresponding to the ground-state hyperfine splitting ($|3\rangle \leftrightarrow |4\rangle$ or $|1\rangle \leftrightarrow |2\rangle$) in Fig. 5) is obtained by modulating the 20% intensity beam with a fibered Mach-Zehnder interferometer (JDS Uniphase X5) driven by a sine wave RF signal supplied by an analog signal generator Agilent E4428C. Through this modulation, two spectral components at $\pm \nu_{rf}$ around the laser frequency ν_L are created in the spectrum of the laser. The probe field is then obtained by filtering the modulated beam using a homemade Fabry-Perot cavity (FPC) locked on the spectral component $\nu_L + \nu_{rf}$ or $\nu_L - \nu_{rf}$ depending on the Λ -like system under investigation. The FPC has a finesse of 260 and a free spectral range of 3.3 GHz. Through a careful mode matching of the incoming beam, we have successfully achieved more than 95% coupling efficiency in the FPC. Before they recombine in the crystal located in the cryostat, the two beams go through AOMs in order to change at will their intensities and their pulse durations. In the gray box of Fig. 7, the sequence applied to the AOM on the optical path of the 80% intensity beam is indicated. A first 60 ms long pulse called pump is applied in order to transfer the populations to the right hyperfine sublevel. The frequency of the pump ν_L is tuned to point A (or B) of Fig. 2 in order to be in resonance with transition $|6\rangle \leftrightarrow |4\rangle$ (or $|5\rangle \leftrightarrow |1\rangle$). 28 ms later a second pulse, the coupling, is applied to the same transition. In the gray box is also indicated both amplitude and frequency evolution of the probe. Most of the time the probe frequency $\nu_L + \nu_{rf}$ is in resonance with transition $|6\rangle \leftrightarrow |3\rangle$ (or $|5\rangle \leftrightarrow |2\rangle$). The probe pulse is turned on a short time after the coupling pulse. Its duration is 50 μ s and its frequency is tuned by few megahertz around the resonance. It is achieved by changing the frequency of the 80 MHz RF signal driving the AOM. The pulse sequence is then repeated at a rate of 1 Hz in order to let a time longer than $T_1^{hyp}=97$ ms for the atomic systems

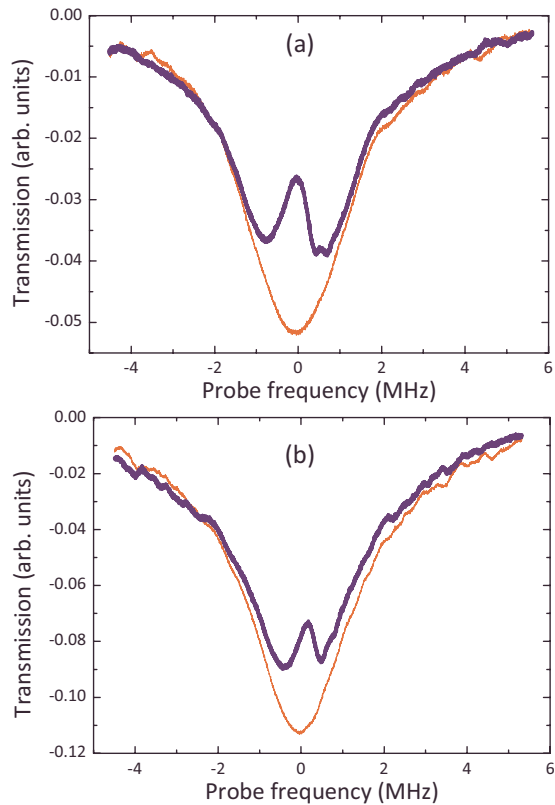


FIG. 8. (Color online) Probe transmission with (thick line) and without (thin line) the control pulse. In both cases the pump is applied 28 ms prior to the control and probe pulses. (a) Observation of EIT in Λ -like system 1. (b) Observation of EIT in Λ -like system 2.

to get back to their initial state between successive measurements.

Figure 8 shows the transmission of the probe as its frequency is tuned by few megahertz around the resonance. The thin line shows the spectrum is obtained when the coupling pulse is not applied. It shows a reduction in the transmission (antiholes in Fig. 5 indicated by the arrows labeled probe) due to population transfer induced by the pump pulse applied to the erbium ions 28 ms prior to the probe pulse. The full width at half maximum (FWHM) of the antihole is about 3.0 MHz. When the coupling pulse is applied simultaneously with the probe a narrow transparency window with a FWHM of about 900 kHz appears at the center of the antihole. It is represented by the thick line in Fig. 8. This relatively narrow transmission peak is attributed to EIT effect. Its amplitude shows an increase in the transmission by about 50% (38%)

for the first (second) Λ -like system relatively to the amplitude of the antihole.

The linewidth of the EIT feature depends on the optical and hyperfine coherences, the intensity of the coupling field, and the inhomogeneous broadening of the hyperfine sublevels. Extra experimental investigations have to be conducted in order to identify precisely the origin of the width of the EIT line. Concerning the amplitude of the EIT, though an increased transmission is observed in our demonstration, the amplitude is still far from reaching the ideal case of an absolute transmission of 100%. This limitation is mainly due, as for the EIT linewidth, to the fact that the coherence of the hyperfine sublevels is finite. However, as pointed out in the introduction, the coherence can be manipulated by reducing the erbium concentration and/or by applying an appropriate external dc magnetic field as it has been successfully achieved in praseodymium-doped crystal.⁵

The present demonstration is achieved without any sophisticated system preparation. This constitutes another significant limitation on the efficiency of the EIT effect since the Λ -like systems under consideration are not ideal closed three-level systems with all population in the sublevel excited by the probe. Indeed, all the fundamental hyperfine sublevels are populated even at 1.5 K. Several techniques can then be implemented in order to prepare more efficiently the systems by having initially all the ions in the hyperfine sublevel on which EIT is observed. This can, for example, be achieved using stimulated Raman adiabatic passage. This process is independent on the spontaneous emission and has been shown to be very efficient^{14,15} in transferring all the population from one ground-state hyperfine sublevel to another hyperfine sublevel without going through optical excitation of the excited state.

IV. CONCLUSION

By using spectral hole burning and electron-paramagnetic-resonance spectroscopies we have studied the hyperfine structure of $^{167}\text{Er}^{3+}$ ions embedded in an Y_2SiO_5 crystalline matrix. Among a large variety of ground-state hyperfine sublevels we have identified 10 Λ -like systems around 1.5 μm . In two of them we have demonstrated an increase in the transparency in a narrow spectral window with a linewidth three times narrower than that of the antihole, feature induced by a pumping process. This effect, clearly associated to EIT, is obtained without implementing any magnetically assisted or sophisticated state preparation. The increase in the transmission associated to EIT, by 50% and 38% depending on the Λ -like system, could be further improved by a better state preparation.

*Corresponding author: kamel.bencheikh@lpn.cnrs.fr; <http://www.lpn.cnrs.fr/>

†Present address: CNAM, 61 rue du Landy, 93210 La Plaine Saint Denis, France.

‡Deceased.

¹M. Fleischhauer, A. Imamoglu, and J. P. Marangos, *Rev. Mod. Phys.* **77**, 633 (2005).

²K. Honda, D. Akamatsu, M. Arikawa, Y. Yokoi, K. Akiba, S. Nagatsuka, T. Tanimura, A. Furusawa, and M. Kozuma, *Phys. Rev. Lett.* **100**, 093601 (2008).

- ³J. Appel, E. Figueroa, D. Korystov, M. Lobino, and A. I. Lvovsky, *Phys. Rev. Lett.* **100**, 093602 (2008).
- ⁴R. M. Macfarlane and R. M. Shelby, *Spectroscopy of Solids Containing Rare Earth Ions* (Elsevier Science BV, North-Holland, 1987), Chap. 3, p. 51.
- ⁵E. Fraval, M. J. Sellars, and J. J. Longdell, *Phys. Rev. Lett.* **95**, 030506 (2005).
- ⁶J. J. Longdell, E. Fraval, M. J. Sellars, and N. B. Manson, *Phys. Rev. Lett.* **95**, 063601 (2005).
- ⁷P. Goldner, O. Guillot-Noël, F. Beaudoux, Y. Le Du, J. Lejay, T. Chanelière, J.-L. Le Gouët, L. Rippe, A. Amari, A. Walther, and S. Kröll, *Phys. Rev. A* **79**, 033809 (2009).
- ⁸E. Baldit, K. Bencheikh, P. Monnier, J. A. Levenson, and V. Rouget, *Phys. Rev. Lett.* **95**, 143601 (2005).
- ⁹T. Böttger, C. W. Thiel, R. L. Cone, and Y. Sun, *Phys. Rev. B* **79**, 115104 (2009).
- ¹⁰O. Guillot-Noël, P. Goldner, Y. Le Du, E. Baldit, P. Monnier, and K. Bencheikh, *Phys. Rev. B* **74**, 214409 (2006).
- ¹¹W. Demtröder, *Laser Spectroscopy* (Springer-Verlag, Berlin, 1996).
- ¹²R. W. P. Drever, J. L. Hall, F. V. Kowalski, J. Hough, G. M. Ford, A. J. Munley, and H. Ward, *Appl. Phys. B: Lasers Opt.* **31**, 97 (1983).
- ¹³T. Böttger, Y. Sun, C. W. Thiel, and R. L. Cone, *Phys. Rev. B* **74**, 075107 (2006).
- ¹⁴J. Klein, F. Beil, and T. Halfmann, *Phys. Rev. Lett.* **99**, 113003 (2007).
- ¹⁵A. L. Alexander, R. Lauro, A. Louchet, T. Chanelière, and J. L. Le Gouët, *Phys. Rev. B* **78**, 144407 (2008).